Effects of Panel Zone Strength and Beam Web Connection Method on Seismic Performance of Reduced Beam Section...

Article *in* Journal of Structural Engineering · December 2005

DOI: 10.1061/(ASCE)0733-9445(2005)131:12(1854)

4 authors, including:

Cheol-Ho Lee
Seoul National University

Chia-Ming Uang
University of California, San Diego

Effects of Panel Zone Strength and Beam Web Connection Method on Seismic Performance of Reduced Beam Section Steel Moment Connections

Cheol-Ho Lee, M.ASCE[1]; Sang-Woo Jeon[2]; Jin-Ho Kim[3]; and Chia-Ming Uang, M.ASCE[4]

Abstract: This paper presents test results on eight reduced beam section (RBS) steel moment connections. The testing program addressed web connection type (bolted versus welded) and panel zone (PZ) strength as the key variables. Specimens with medium PZ strength were designed to promote energy dissipation from both PZ and RBS regions such that expensive doubler plates were not needed. Both strong and medium PZ specimens with a welded web connection were able to provide satisfactory connection rotation capacity for special moment-resisting frames. However, specimens with a bolted web connection performed poorly due to premature brittle fracture of the beam flange at the weld access hole. A plausible explanation for the higher incidence of base metal fracture in bolted web specimens was presented based on the measured strain data. Test results from this study and by others showed that panel zones could easily develop a plastic rotation of 0.01 rad without causing distress to the beam flange groove welds. At this deformation level, the amount of beam distortion (i.e., buckling) was about one half that developed in strong PZ specimens. A criterion for a balanced PZ strength that improves the plastic rotation capacity while reducing the amount of beam buckling is proposed.

DOI: 10.1061/(ASCE)0733-9445(2005)131:12(1854)

CE Database subject headings: Connections; Beams; Steel frames; Seismic design; Design criteria; Moments.

Introduction

In response to the widespread damage in connections of steel moment-resisting frames that was observed after the 1994 Northridge, Calif. and the 1995 Kobe, Japan earthquakes, a number of improved beam-to-column connection design strategies have been proposed. Of a variety of new designs, the reduced beam section (RBS) connection has been shown to exhibit satisfactory levels of ductility in numerous tests and has found broad acceptance in a relatively short time (Chen et al. 1996; Plumier 1997; Zekioglu et al. 1997; Engelhardt et al. 1998). In RBS connections a portion of the beam flanges at a short distance from the column face is strategically trimmed to promote stable yielding at the reduced section and to effectively protect the more vulnerable welded joints. This weakening strategy also reduces the seismic force demand in the column and the panel zone. Although this type of moment connection has been widely used after the Northridge earthquake, several design issues still remain (for example, Chi and Uang 2002; Jones et al. 2002). Issues that require further examination include the influence of the beam web connection method and panel zone strength on the seismic performance of RBS connections.

Most of the past tests on RBS moment connections used a fully welded beam web. Recent tests conducted by Jones et al. (2002) showed that while specimens with either bolted or welded web connections generally achieve acceptable performance, specimens with bolted web connections exhibited a higher incidence of fractures in close proximity to the welds. Their tests, consistent with other past RBS tests, indicated that the use of welded web does provide some benefit to connection performance. However, consensus does not seem to exist on whether a bolted web attachment can be used reliably in lieu of a welded web attachment for the prequalified RBS connections.

Another issue is the optimal panel zone strength. Engelhardt et al. (1998) conducted tests that included an evaluation of the effect of panel zone yielding on the performance of RBS connections. Jones et al. (2002) reported test results based on specimens with very weak to very strong panel zones. Although a significant amount of RBS test data is available, a specific recommendation for a desirable range of panel zone strength has yet to be proposed. The first objective of this study was to further investigate the effect of the beam web connection method and the panel zone strength on RBS connection performance. The second objective was to propose a balanced panel zone strength criterion based on the test results from this study and by others.

Testing Program

Design of Test Specimens

A total of eight full-scale test specimens were designed and grouped as Set numbers 1 and 2 (Table 1). Typical geometry and

[1]Associate Professor, Dept. of Architecture, Seoul National Univ., Seoul 151-742, Korea (corresponding author). E-mail: ceholee@snu.ac.kr

[2]Research Engineer, Research Institute of Industrial Science and Technology, Kyung-gi 455-810, Korea. E-mail: jswsy@rist.re.kr

[3]Research Engineer, Research Institute of Industrial Science and Technology, Kyung-gi 455-810, Korea. E-mail: jhkim@rist.re.kr

[4]Professor, Dept. of Structural Engineering, Univ. of California at San Diego, La Jolla, CA 92093-0085. E-mail: cmu@ucsd.edu

Note. Associate Editor: Gregory A. MacRae. Discussion open until May 1, 2006. Separate discussions must be submitted for individual papers. To extend the closing date by one month, a written request must be filed with the ASCE Managing Editor. The manuscript for this paper was submitted for review and possible publication on May 22, 2003; approved on March 16, 2005. This paper is part of the ***Journal of Structural Engineering***, Vol. 131, No. 12, December 1, 2005. ©ASCE, ISSN 0733-9445/2005/12-1854–1865/$25.00.

J. Struct. Eng., 2005, 131(12): 1854-1865

Table 1. Test Specimens

Specimen	Beam and column (equivalent US *W* section)	PZ strength ratio[a]	Beam web connection method	*a* (mm)	*b* (mm)	*c* (mm)	Flange reduction (%)
			Set number 1				
DB700-SW	$H700\times300\times13\times24$ $(W27\times123)$ $H428\times407\times20\times35$ $(W17\times271)$	Strong (not available)	Welded	175	525	55	37
DB700-MW	$H700\times300\times13\times24$ $(W27\times123)$ $H428\times407\times20\times35$ $(W17\times271)$	Medium (0.87)	Welded	175	525	55	37
DB700-SB	$H700\times300\times13\times24$ $(W27\times123)$ $H428\times407\times20\times35$ $(W17\times271)$	Strong (not available)	Bolted	175	525	55	37
DB700-MB	$H700\times300\times13\times24$ $(W27\times123)$ $H428\times407\times20\times35$ $(W17\times271)$	Medium (0.87)	Bolted	175	525	55	37
			Set number 2				
DB600-MW1	$H600\times200\times11\times17$ $(W24\times70)$ $H400\times400\times13\times21$ $(W16\times115)$	Medium (0.83)	Welded	150	510	40	40
DB600-MW2	$H600\times200\times11\times17$ $(W24\times70)$ $H400\times400\times13\times21$ $(W16\times115)$	Medium (0.82)	Welded	150	390	40	40
DB600-SW1	$H600\times200\times11\times17$ $(W24\times70)$ $H588\times300\times12\times20$ $(W24\times100)$	Strong (0.66)	Welded	150	450	40	40
DB600-SW2	$H606\times201\times12\times20$ $(W24\times80)$ $H588\times300\times12\times20$ $(W24\times100)$	Strong (0.63)	Welded	150	450	40	40

[a]Based on the strength ratio $V_{\mathrm{RBS},p}/V_p$; refer to Eqs. (4) and (8) for definition.

seismic moment profile for the design of the radius-cut RBS are shown in Figs. 1 and 2. The grade of steel for the beams was SS400 with a specified minimum yield strength of 235 MPa (34 ksi); SM490 steel was used for the columns and the specified minimum yield strength was 324 MPa (47 ksi). The tensile coupon test results are summarized in Table 2. The RBS design followed the recommendations by Iwankiw (1997) and Engelhardt et al. (1998). The beam end length (a) and the total length of the RBS zone (b) were chosen to be 58–75% of the beam flange width and 75% of the beam depth, respectively. The strain hardened plastic moment at the RBS hinge was calculated using the expected yield strength ($F_{\mathrm{ye}}=R_y\times F_y=1.33\times235=313$ MPa) and a strain hardening factor of 1.1

$$m_p^{\mathrm{act}}=\alpha\times Z_{\mathrm{RBS}}\times F_{\mathrm{ye}}=(1.1)\times Z_{\mathrm{RBS}}\times F_{\mathrm{ye}} \tag{1}$$

The corresponding seismic moment at the face of the column is

$$M_f=m_p^{\mathrm{act}}\left(\frac{L_b}{L'}\right) \tag{2}$$

Engelhardt et al. (1998) recommended that the moment, M_f, at the face of the column be limited to approximately 85–100% of M_p, where M_p=expected plastic moment of the unreduced beam section. In this study the trimmed flanges were sized to limit the moment at the column face to about 90% of M_p. The reduction in flange area at the RBS center was 37 and 40% for Set numbers 1 and 2, respectively (see Table 1). The flange reduction in Set number 1 was slightly less than the 40% minimum reduction as suggested by the SAC recommendation (SAC 2000).

The panel zones were then designed by using either of the following two equations for the panel zone design shear strength:

$$V_p=(0.75)(0.6F_{\mathrm{yc}}d_ct_p)\left[1+\frac{3b_{\mathrm{cf}}t_{\mathrm{cf}}^2}{d_bd_ct_p}\right] \tag{3}$$

J. Struct. Eng., 2005, 131(12): 1854-1865

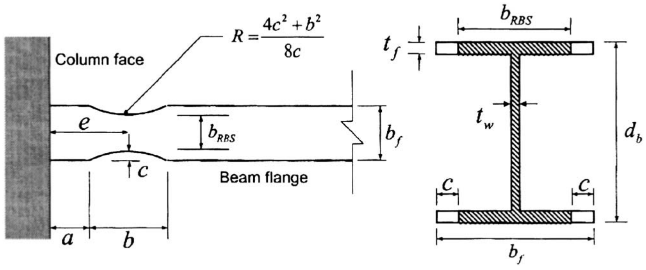

Fig. 1. Typical geometry of radius-cut reduced beam section

$$V_p = (0.6F_{\mathrm{yc}}d_ct_p)\left[1 + \frac{3b_{\mathrm{cf}}t_{\mathrm{cf}}^2}{d_bd_ct_p}\right] \quad (4)$$

where F_{yc}=yield strength of the column; d_b=beam depth; d_c=column depth; t_p=thickness of the panel zone; b_{cf}=column flange width; and t_{cf}=column flange thickness. Eq. (4), which is adopted in the 2002 AISC Seismic Provisions, was used to design the medium panel zone specimens. This equation represents the panel zone shear strength when the shear strain reaches four times the shear yield strain (Krawinkler 1978). Eq. (3), which includes a strength reduction factor of 0.75, was implemented in the 1997 AISC Seismic Provisions. Specimens with panel zone designed by Eq. (3) are defined as the strong panel zone specimens in this study because inelastic rotation is expected to develop mainly in the beam. In Set number 1, identical sections were used for the beams and columns, respectively. When Eq. (3) was used for the panel zone strength, a doubler plate of 10 mm thickness was provided for specimens *DB700-SB* and *DB700-SW*. The doubler plate was plug-welded to the column web to prevent premature local buckling (AISC 1997).

To estimate the required shear strength of the panel zone, it is worth noting that a reduction factor of 0.8 on beam yielding was included in the 1997 AISC Seismic Provisions to account for the effect that gravity loads might inhibit the simultaneous formation of plastic hinges on both sides of a column. Since there is no assurance that this will be the case, especially for one-sided connections and for perimeter frames where gravity loads may be relatively small, the 2002 AISC Seismic Provisions requires that the expected shear demand in the panel zone be calculated from the summation of the moments at the column faces, as determined by projecting the expected moments at the plastic hinge points to the column faces without considering the presence of gravity moments.

Four medium panel zone specimens were included in this testing program (*DB700-MW* and *DB700-MB* in Set number 1, *DB600-MW1* and *DB600-MW2* in Set number 2). Specimens *DB600-MW1* and *DB600-MW2* in Set number 2 were identical, except for a slight difference in the RBS length. The RBS length was taken as 85 and 65% of the beam depth for *DB600-MW1* and *DB600-MW2*, respectively.

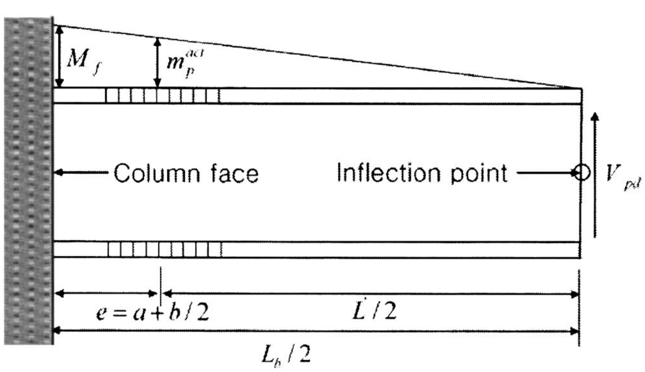

Fig. 2. Seismic moment profile for reduced beam section design

Table 2. Tensile Coupon Test Results

Member	Coupon	Yield strength (MPa)	Tensile strength (MPa)	Yield ratio (%)
Beam ($W27\times123$)	Flange	304	455	67
$H700\times300\times13\times24$ (SS400)	Web	364	480	76
Column ($W17\times271$)	Flange	343	512	67
$H428\times407\times20\times35$ (SM490)	Web	358	520	69
Beam ($W24\times70$)	Flange	326	467	70
$H600\times200\times11\times17$ (SS400)	Web	343	473	73
Column ($W16\times115$)	Flange	358	525	68
$H400\times400\times13\times21$ (SM490)	Web	374	531	74
Beam ($W24\times80$)	Flange	295	447	66
$H606\times201\times12\times20$ (SS400)	Web	333	471	71
Column ($W23\times100$)	Flange	374	534	70
$H588\times300\times12\times20$ (SM490)	Web	405	546	74

Most of the past tests on RBS moment connections used a fully welded beam web. Recently, Jones et al. (2002) indicated that the use of a welded web connection does provide some benefit to the connection performance as it tends to reduce the vulnerability of the weld fracture. To further investigate the influence of beam web connection, two bolted web specimens, *DB700-SB* and *DB700-MB*, were included in Set number 1. The bolted web connection consisted of eight fully tensioned *M22-F10T* high-strength bolts. The bolts were tightened with the calibrated wrench method with a specified bolt tension of 201 kN. In Set number 2, all the beam webs were groove welded to the column flange.

Continuity plates equal in thickness to the beam flange were provided in all specimens. Electrodes with a specified minimum Charpy V-Notch (CVN) toughness of 26.7 J at −28.9°C (20 lbf at −20°F) was specified for flux-cored arc welding. Weld access hole configurations followed the SAC recommendations (SAC 2000). Figs. 3 and 4 show the connection details for specimens *DB700-SW* and *DB700-SB*. In Table 1, the following abbreviations were used for the specimen designation: *S*=strong panel zone, *M*=medium panel zone, *W*=welded web, and *B*=bolted web.

Test Setup and Loading

The specimens were mounted to a strong floor and a strong wall. An overall view of the test setup is shown in Fig. 5. Lateral restraint was provided at a distance of 2,500 mm from the column face. The specimens were tested statically according to the SAC standard loading protocol as shown in Fig. 6 (Krawinkler et al. 2000). The test specimens were instrumented with a combination

J. Struct. Eng., 2005, 131(12): 1854-1865

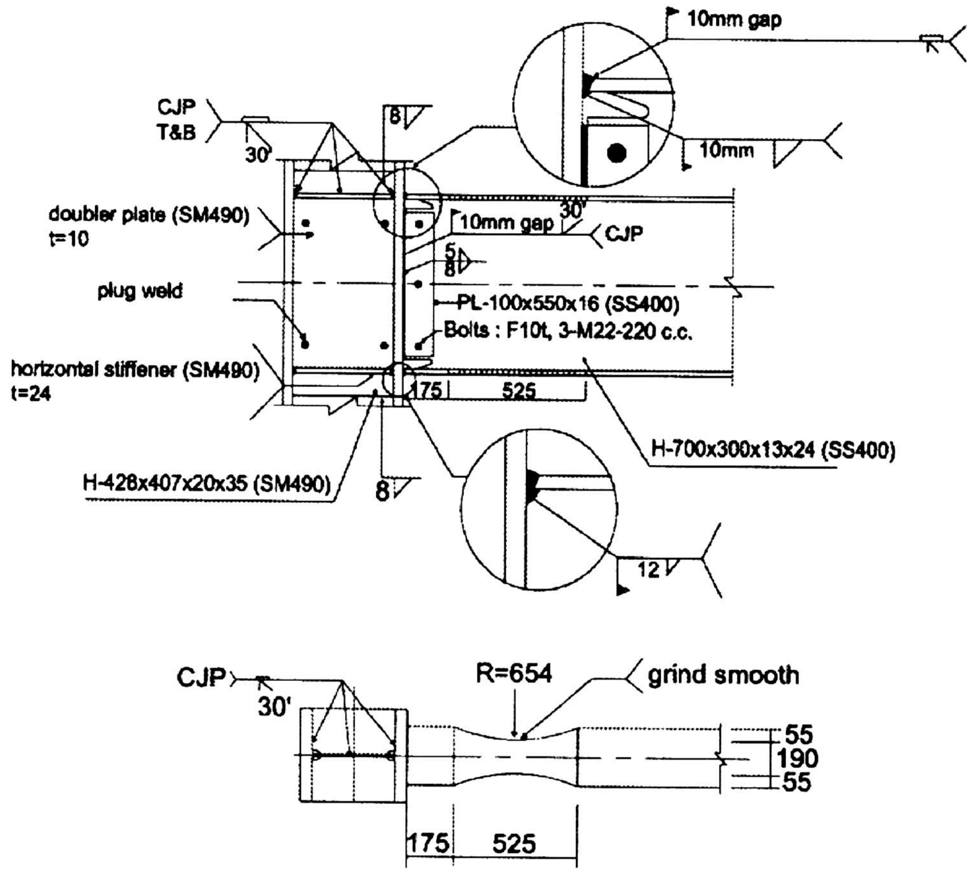

Fig. 3. Specimen *DB700-SW* moment connection details

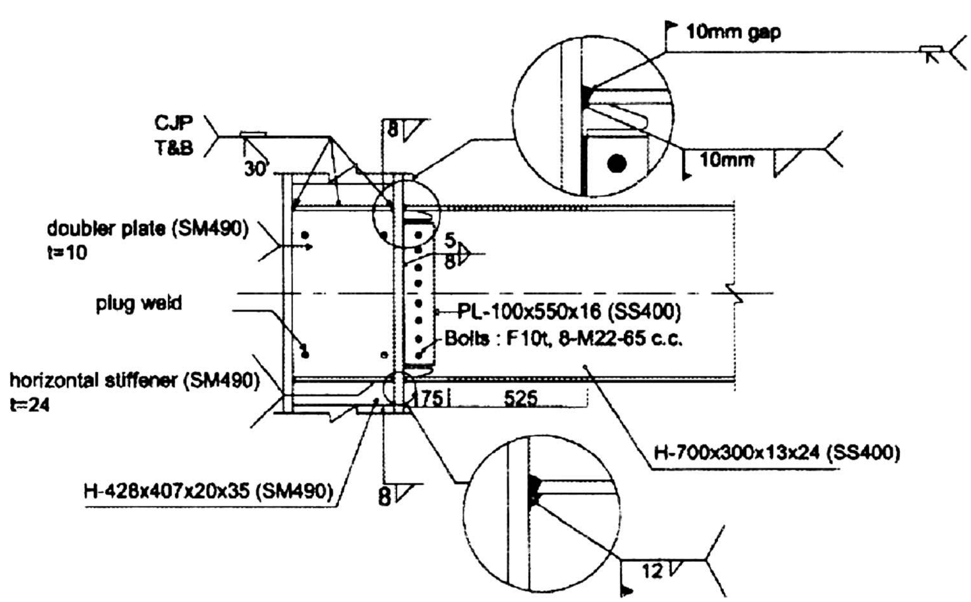

Fig. 4. Specimen *DB700-SB* moment connection details

J. Struct. Eng., 2005, 131(12): 1854-1865

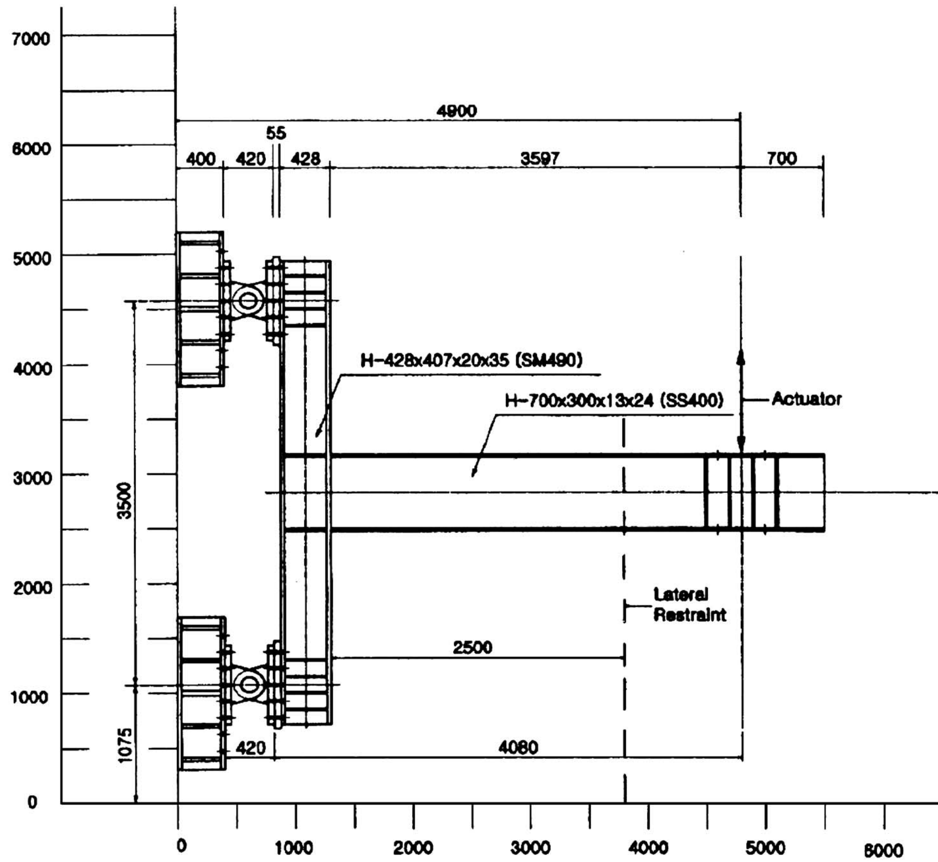

Fig. 5. Test setup

of displacement transducers and strain gages to measure global and local responses. Whitewash was painted in the connection region to monitor yielding.

Test Results and Discussion

The cyclic responses of the specimens in Set number 1 are presented in Fig. 7. The ordinate is expressed in terms of the normalized moment at the column face; the normalization was based on the nominal plastic moment of the unreduced beam section. Both strong and medium panel zone specimens with a welded web connection developed satisfactory levels of ductility (4% drift) required for special moment frames. Figs. 8 and 9 show the plastic hinge formation in the welded web specimens. Significant yielding of the panel zone in Specimen *DB700-MW* was evident from the flaking of the whitewash. Specimen *DB700-SW* exhibited excellent rotation capacity without fracture. But specimens with a bolted web connection performed poorly due to brittle fracture across the beam flange at the weld access hole (see Figs. 10 and 11).

Fig. 12 shows a comparison of the normalized maximum moment at the centerline of the RBS (i.e., the assumed plastic hinge location). The moment was normalized by the plastic moment of

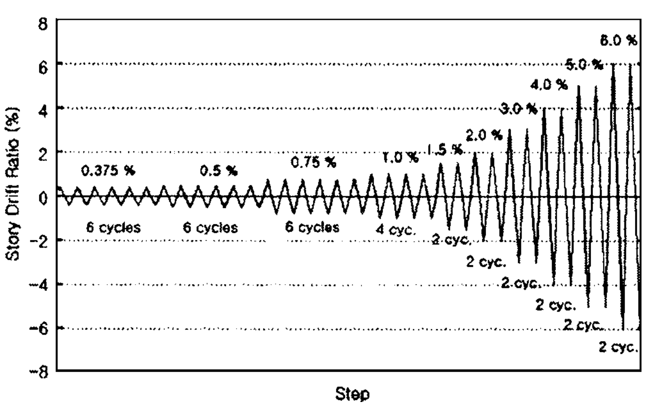

Fig. 6. SAC standard loading history

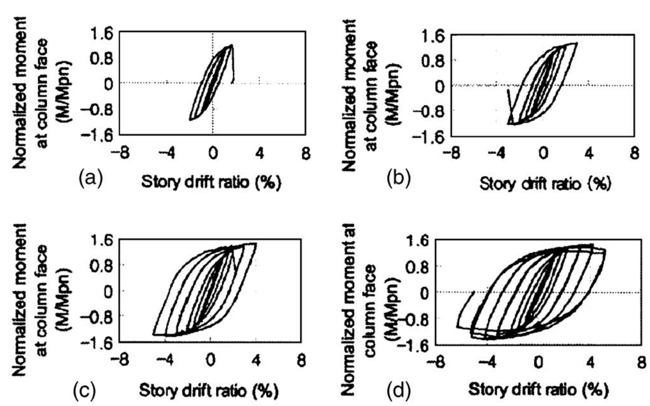

Fig. 7. Normalized moment versus story drift ratio relationship (set number 1): (a) *DB700-SB*, (b) *DB700-MB*, (c) *DB700-MW*, and (d) *DB700-SW*

J. Struct. Eng., 2005, 131(12): 1854-1865

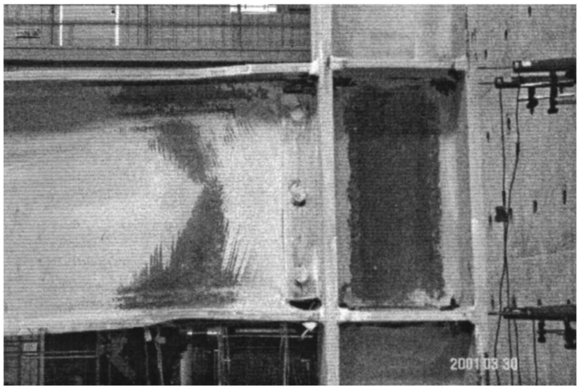

Fig. 8. Connection region of specimen *DB700-MW* at 5% story drift

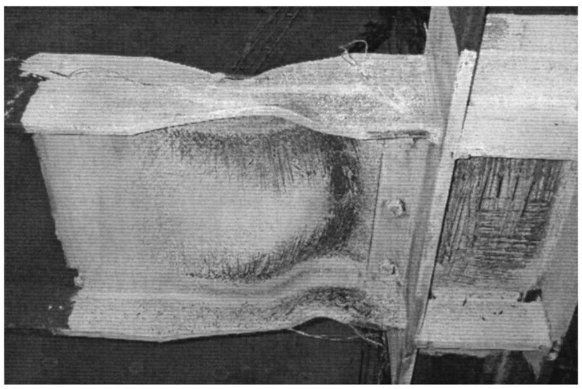

Fig. 9. Connection region of specimen *DB700-SW* at 6% story drift

Fig. 10. Beam bottom flange fracture of specimen *DB700-SB* at 2% story drift

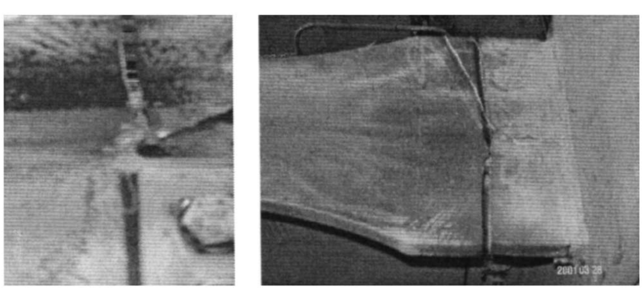

Fig. 11. Beam top flange fracture of specimen *DB700-MB* at 3% story drift

the narrowest reduced beam section based on the measured yield strength. For a given story drift ratio, the figure shows that the maximum moment developed in the bolted web specimens were slightly less. Fig. 13 compares the measured flexural strains of Specimens *DB700-SB* and *DB700-SW* near the groove weld of the beam bottom flange up to the drift level when *DB700-SB* fractured. Much higher strain in the bolted web specimen is evident. This suggests the possibility of web bolt slippage. Indeed, bolt slippage was consistently observed during the past test of pre-Northridge (welded flange and bolted web) connections (Krawinkler and Popov 1982; Tsai and Popov 1988; Ricles et al. 2002). This bolt slippage was considered as having contributed to the weld fractures observed in most specimens with this type of connection. In the test conducted by Tsai and Popov (1988), the improved performance of the connection was attained when either beam web-to-shear tab welding or tension control web bolts, both of which helped prevent the web bolt slippage, was used.

Fig. 14 shows that all welded-web specimens in Set number 2 exhibited satisfactory connection ductility. Fig. 15 presents a comparison of the measured beam lateral–torsional buckling (LTB) amplitudes up to the 4% story drift cycles. The LTB amplitudes were measured based on the buckled flange shape. Because panel zone contributed less to plastic rotation in the strong panel zone specimens, LTB amplitudes of these beams were larger. Since a well designed RBS connection would fracture eventually by low-cycle fatigue of the beam flanges in the RBS region for drift beyond 4% and such fracture is associated with very large curvatures due to buckling, a reduction of the LTB amplitude implies both less postearthquake damage and a less tendency for beam flange fracture. Fig. 16 shows a plot similar to Fig. 12, but for all welded-web specimens. The figure shows that the normalized maximum moment (i.e., cyclic strain hardening factor) reached an average value of 1.27 at 4% story drift. This value is higher than that assumed (1.1 in the AISC Seismic Provisions and 1.15 in *FEMA 350*) for design.

Effects of Panel Zone Strength

For the purpose of analyzing the effects of panel zone strength, Krawinkler's recommendation [Eq. (4)], which includes the column flange contribution (CFC) to the postyield strength, was used as a measure of the panel zone strength. The first term in Eq. (4) represents the first yielding of the column panel zone (or the von

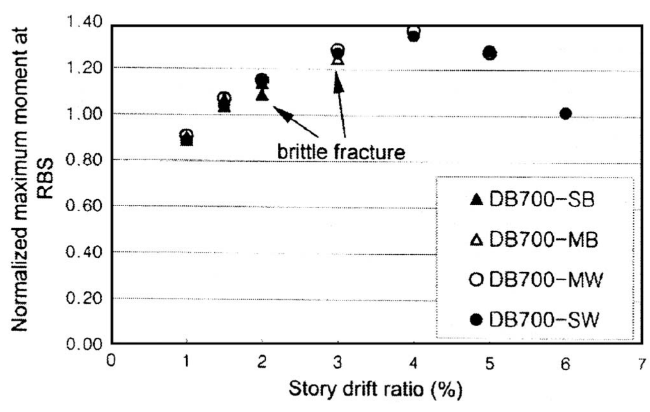

Fig. 12. Comparison of normalized maximum moment at reduced beam section (Set number 1)

J. Struct. Eng., 2005, 131(12): 1854-1865

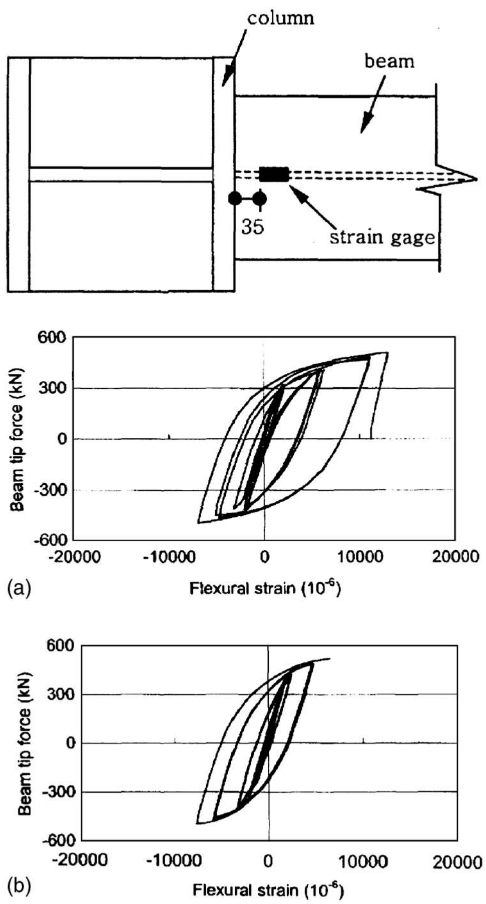

Fig. 13. Comparison of measured flexural strain responses near groove weld of beam bottom flange: (a) *DB700-SB* and (b) *DB700-SW*

Mises yield criterion). The ratio of the second term over the first term inside the parentheses represents the increase in panel zone shear resistance beyond that predicted by the von Mises yield criterion. Heavy columns with thicker and wider flanges will benefit more from the higher resistance provided by this second term. Eq. (4) can be expressed in terms of the von Mises strength (V_y) and the CFC as follows:

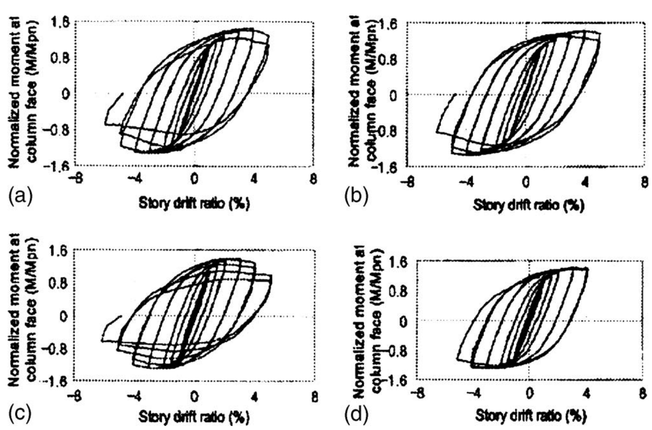

Fig. 14. Normalized moment versus story drift ratio relationship (set number 2): (a) *DB600-MW1*, (b) *DB600-MW2*, (c) *DB600-SW1*, and (d) *DB600-SW2*

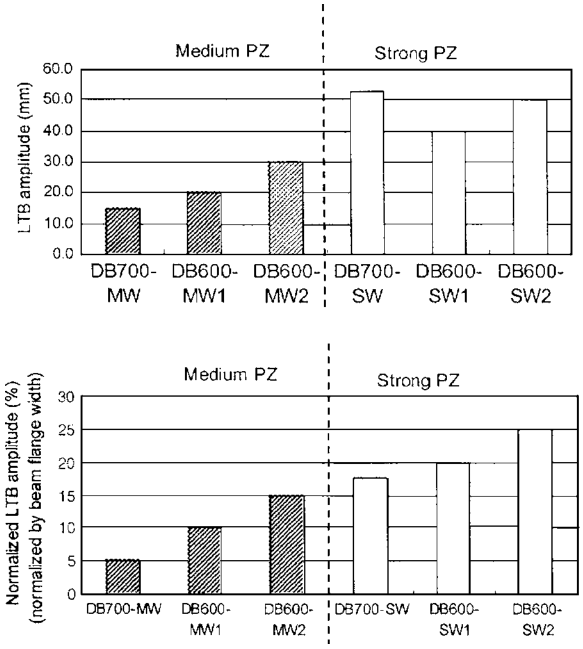

Fig. 15. Comparison of lateral–torsional buckling amplitudes at 4% story drift cycle: (a) absolute amplitude and (b) relative amplitude

$$V_p = V_y(1 + \mathrm{CFC}) \tag{5}$$

where

$$V_y = \frac{1}{\sqrt{3}}F_{\mathrm{yc}}d_c t_p \approx 0.6F_{\mathrm{yc}}d_c t_p \tag{6}$$

and

$$\mathrm{CFC} = \frac{3b_{\mathrm{cf}}t_{\mathrm{cf}}^2}{d_b d_c t_p} \tag{7}$$

As a measure of the beam strength, the panel zone shear force $V_{\mathrm{RBS},p}$ corresponding to the development of the actual plastic moment of the RBS was used; such a measure was also used by Roeder (2002). For a one-sided moment connection, $V_{\mathrm{RBS},p}$ can be computed as follows:

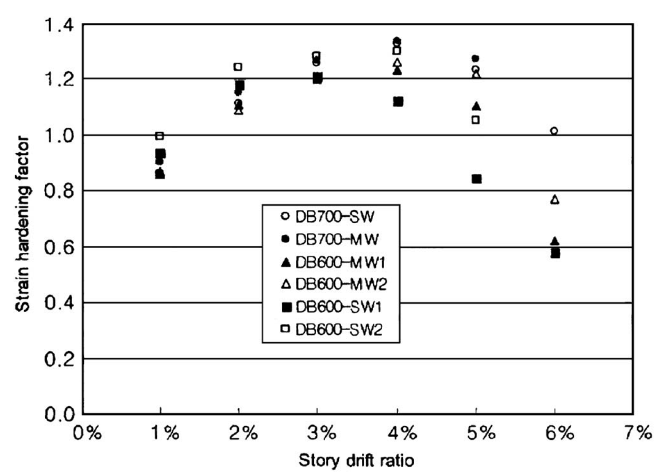

Fig. 16. Story drift ratio versus strain hardening factor in welded-web specimens

J. Struct. Eng., 2005, 131(12): 1854-1865

Table 3. Effects of Panel Zone Strength on Plastic Rotation and Energy Dissipation

(a) One-sided moment connection tests

Specimen (beam and column sizes)	PZ strength ratio ($V_{\mathrm{RBS},p}/V_p$)	Panel zone plastic rotation at 4% story drift ratio (rad)	Energy dissipation by panel zone up to 4% story drift cycle (%)
DB700-MW (*W*27×123 and *W*17×271)	0.87	0.012	43
DB600-MW1 (*W*24×70 and *W*16×115)	0.83	0.008	32
DB600-MW2 (*W*24×70 and *W*16×115)	0.82	0.009	30
RB5[a] (*W*24×70 and *W*12×125)	0.82	0.011	37
RB1[a] (*W*24×70 and *W*12×125)	0.77	0.010	33
LS1[b] (*W*30×99 and *W*14×176)	0.76	0.008	28
DB5[c] (*W*30×148 and *W*14×257)	0.72	0.01 rad out of total plastic rotation of 0.04 rad	Not available
DC2[d] (*W*36×150 and *W*14×150)	0.67	0.005	24
DB600-SW1 (*W*24×70 and *W*24×100)	0.66	0.0002	5
DB600-SW2 (*W*24×80 and *W*24×100)	0.63	Negligible	Negligible

(b) Two-sided moment connection tests[e]

		Energy dissipation[f]				
Specimen (column size)	PZ strength ratio $V_{\mathrm{RBS},p}/V_p$	Total (kJ)	Dissipated by beams (kJ)	Dissipated by panel zone (kJ)	Dissipated by columns (kJ)	Panel zone plastic rotation (rad)
1B (*W*14×398)	0.91 (bare steel, balanced PZ)	2,572	1,991 (75%)[f]	456 (25%)[f]	125	0.005
1C (*W*14×398)	0.91 (composite slab, balanced PZ)	5,631	3,805 (45%)[f]	1,594 (55%)[f]	232	0.010
3B[g] (*W*14×283)	1.40 (bare steel, very weak PZ)	3,915	937 (24%)	2,559 (65%)	419 (11%)	0.034
3C[g] (*W*14×283)	1.40 (composite slab, very weak PZ)	6,041	19 (0%)	5,068 (84%)	954 (16%)	0.038
4B (*W*14×398 column with two 19 mm doubler plates)	0.56 (bare steel, very strong PZ)	1,430	1,400 (98%)	30 (2%)	—	Negligible
4C (*W*14×398 column with two 19 mm doubler plates)	0.56 (composite slab, very strong PZ)	3,511	3,482 (99%)	37 (1%)	—	Negligible

[a]From Tsai and Chen (2000).

[b]From Yu et al. (2000).

[c]From Engelhardt et al. (1998): the cyclic loading history was slightly different from the SAC standard loading protocol.

[d]From Chi and Uang (2002).

[e]From Engelhardt et al. (2000) and Jones et al. (2002). All specimens were provided with *W*36×150 beams (A572 Grade 50 steel) and all the columns were provided with A572 Grade 50 steel.

[f]Energy dissipation up to 4% story drift cycles.

[g]Column plastic rotation of about 0.008 rad occurred in these specimens.

J. Struct. Eng., 2005, 131(12): 1854-1865

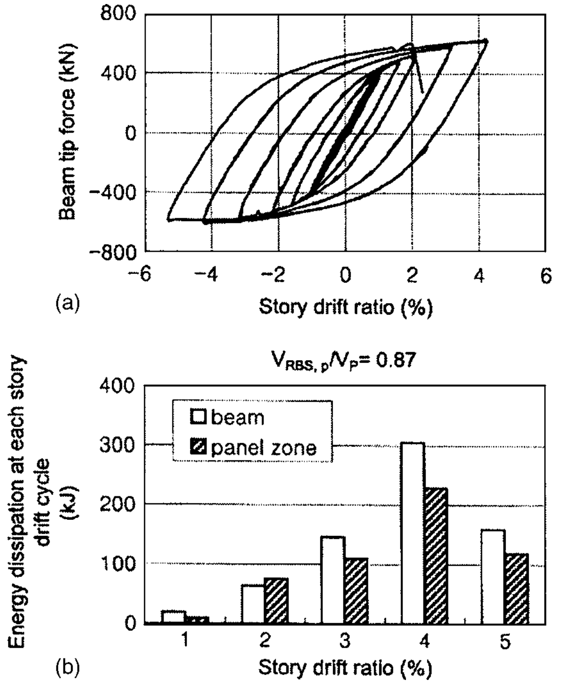

Fig. 17. Global response and energy dissipation (specimen *DB700-MW*): (a) global response and (b) energy dissipation at each story drift cycle

$$V_{\mathrm{RBS},p} = \left(\frac{M_{\mathrm{RBS},p}}{d_b}\right) \times \left(\frac{L_b/2 + d_c/2}{L_b/2 - e}\right) \times \left(1 - \frac{d_b}{H_c}\right) \tag{8}$$

where $M_{\mathrm{RBS},P}$=plastic moment at the RBS based on the measured yield strength; and H_c=column height. Refer to Fig. 2 for the remaining symbols. For a two-sided moment connection configu-

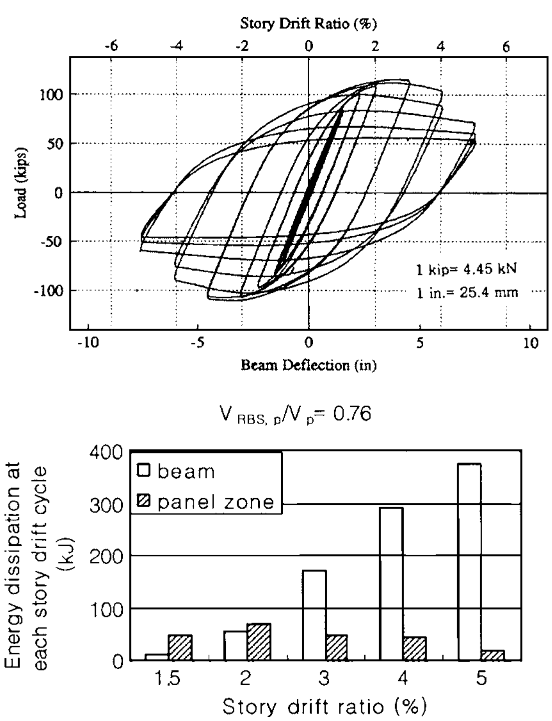

Fig. 18. Global response and energy dissipation at each story drift cycle (specimen *LS1*)

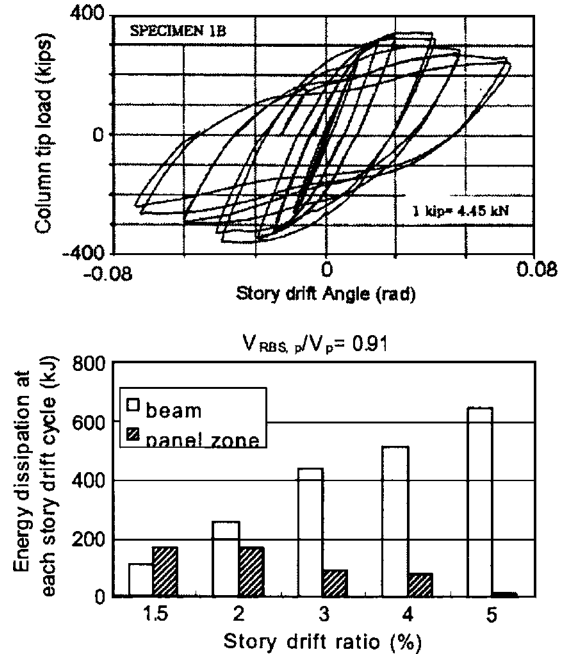

Fig. 19. Global response and energy dissipation at each story drift cycle (specimen *IB*)

ration with the same beam size and span length on both sides of the column, $V_{\mathrm{RBS},p}$ is twice the value given by Eq. (8). Once the beam strength is expressed in the form of $V_{\mathrm{RBS},p}$, the relative strength between the beam and the panel zone can be measured by the ratio $V_{\mathrm{RBS},p}/V_p$; a lower value implies a stronger panel zone.

The effects of panel zone strength on some connection responses are summarized in Table 3. Specimen *DB700-SW* was excluded from Table 3 because the tensile coupon test results for

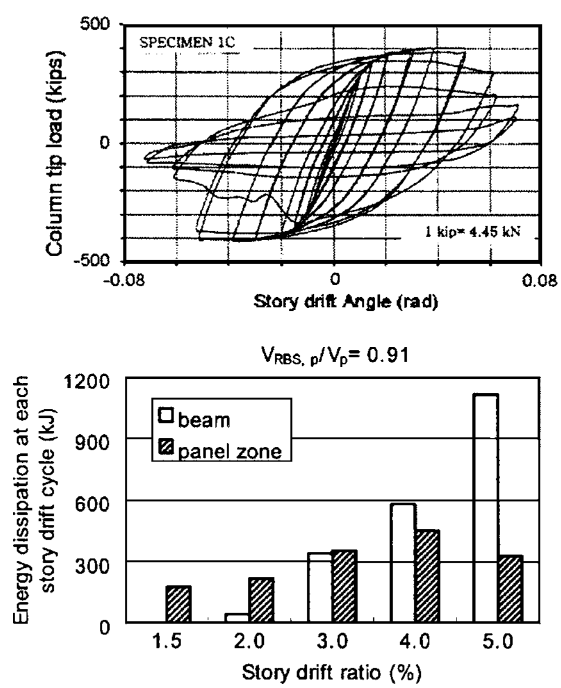

Fig. 20. Global response and energy dissipation at each story drift cycle (specimen *1C*)

J. Struct. Eng., 2005, 131(12): 1854-1865

the doubler plates were not available. To augment the database, test results from Engelhardt et al. (1998, 2000), Tsai and Chen (2000), Yu et al. (2000), Chi and Uang (2002), and Jones et al. (2002) were included. Table 3(a) summarizes one-sided moment connection tests with bare steel specimens. Table 3(b) summarizes two-sided moment connection tests conducted by Engelhardt et al. (2000) and Jones et al. (2002) to investigate the effect of column panel zone strength and composite floor slab. The test data in the table comprise specimens with various column and beam sizes; all specimens were able to develop satisfactory connection rotation capacity for special moment-resisting frames. The measured yield strength was used in calculating the relative panel zone strength in Table 3. The panel zone strength ranges from very weak to very strong. Several observations from the data in Table 3 are summarized in the following subsection.

Energy Dissipation and Plastic Rotation by Panel Zone

First, it is noted from Table 3(a) that the one-sided moment connection specimens with a weaker panel zone consistently dissipated more energy through panel zone yielding. Up to 4% story drift cycle, specimens with $V_{\mathrm{RBS},p}/V_p=0.70-0.90$ developed about 0.01 rad plastic rotation and dissipated about 30–40% of the total energy.

Global response and energy dissipation behavior of the four specimens selected from Table 3 are presented in Figs. 17–20. The panel zone in Specimen *DB700-MW* ($V_{\mathrm{RBS},p}/V_p=0.87$) dissipated 43% of the total energy up to 4% story drift cycle. The panel zone of Specimen *LS1*, which had a relatively stronger panel zone ($V_{\mathrm{RBS},p}/V_p=0.76$) as compared to Specimen *DB700-MW*, dissipated 28% of the total energy and developed a panel zone plastic rotation of 0.008 rad. However, Specimen *1B* ($V_{\mathrm{RBS},p}/V_p=0.91$), which possessed a panel zone slightly weaker than that of Specimen *DB700-MW*, showed a much lower (25%) energy dissipation by the panel zone. Such inconsistency is due to cyclic instability, as explained below.

Table 4 summarizes the slenderness ratios and the limiting values for the four specimens. Of the three buckling limit states, it was shown by Uang and Fan (2001) that web local buckling (WLB) was the dominating mode for RBS beams. Table 4 shows that Specimen *DB700-MW* satisfied all the AISC seismic requirements for stability. Specimen *LS1* violated the LTB and flange local buckling (FLB) requirements by a small margin. But Specimen *1B* violated the LTB requirement by a large margin. As a result, the beam strength degraded beyond 3% drift (Fig. 19). Since the beam did not have sufficient strength to mobilize the panel zone at higher drift levels, energy dissipation of the latter is low. It is expected that the energy dissipation of the panel zone would be increased had the beams properly braced. This can be demonstrated by examining the cyclic performance of Specimen *1C*.

Specimen *1C* was nominally identical to *1B*, except that the former incorporated a concrete slab. Although Specimen *1C*, like *1B*, also did not satisfy the LTB requirement (Table 4), the bracing effect provided by the slab is obvious (Fig. 20). The specimen was able to reach 5% drift before significant strength degradation started to occur. The panel zone was sufficiently mobilized for yielding, and it dissipated 55% of the total energy up to 4% drift cycles. The plastic rotation developed in the panel zone was 0.01 rad, which is comparable to that developed in Specimen *DB700-MW*. It is worthwhile to note from Table 3(b) that composite specimens exhibited a greater strength (about 10% on average) and energy dissipation (often more than twice) than their bare steel counterparts.

Behavior of Specimens with Very Strong or Very Weak Panel Zones

Two specimens (*4B* and *4C*) in Table 3(b) that were designed for a strong panel zone ($V_{\mathrm{RBS},p}/V_p=0.56$) dissipated a considerably less amount of energy than the other specimens. One consequence of the strong panel zone design was that all energy dissipation was concentrated in the RBS region, while caused a significant amount of buckling. Lateral–torsional buckling of the beams then caused column twisting (Engelhardt et al. 2000; Chi and Uang 2002; Jones et al. 2002), thus preventing the specimens from developing sufficient ductility.

The problem of strong panel zone design mentioned above can be somewhat alleviated if the panel zone is also designed to yield. In the extreme case, a very weak panel zone design would result in a situation where the beam would remain elastic while all the inelasticity action occurs in the panel zone. This was the case for Specimens *3B* and *3C* in Table 3(b); both specimens showed very stable hysteretic response before the beams fractured at large drift levels. The plastic rotation developed in the panel zone ranged from 0.034 to 0.038 rad. Large rotations in the panel zone were accompanied by kinking of the column flanges at the four corners of the panel zone.

Tests on free flange moment connection conducted by Choi et al. (2000) also revealed similar problems associated with the very weak or very strong panel zone design; excessive panel zone yielding of the weak panel zone specimens eventually fractured the beam flange while severe out-of-plane deformation was observed in the strong panel zone specimens.

Table 4. Comparison of Slenderness Ratios

	Buckling mode					
	Web local buckling (WLB)		Lateral torsional bucking (LTB)		Flange local buckling (FLB) (unreduced section)	
Specimen	h/t_w	Limit[a]	L_b/r_y	Limit[b]	$b_f/(2t_f)$	Limit[c]
DB700-MW	46 (80% of limit)	57	37 (66% of limit)	56	6.3 (81% of limit)	7.8
LS1	51 (89% of limit)	57	47.6 (9% over)	44	7.8 (10% over)	7.1
1B, *1C*	53 (98% of limit)	54	63 (37% over)	46	6.4 (90% of limit)	7.1

[a] $1{,}100/\sqrt{F_y}$ (F_y in MPa): based on the recommendation by Uang and Fan (2001).

[b] $6{,}560/F_y$ (F_y in MPa).

[c] $136/\sqrt{F_y}$ (F_y in MPa).

J. Struct. Eng., 2005, 131(12): 1854-1865

Although weak panel zone design has been studied (Kawano 1984; Suita et al. 2002) and available test data showed stable cyclic response, this design approach is not favored for the welded moment connection design for the following concerns. First, kinking of the column flanges not only produces complex triaxial stress conditions but also increases the potential for fracture in the beam flange welds (El-Tawil 2000). Second, weak panel zone design would result in a lower system overstrength of the structure; system overstrength plays an important role in the survival of a structure during a major earthquake (Uang 1993).

Proposed Balanced Design Criteria

Based on the data presented in Table 3, a balanced panel zone strength ratio can be developed such that problems associated with the use of either a strong or a weak panel zone can be avoided. It was shown that a properly designed panel zone can easily develop a plastic rotation of about 0.01 rad and dissipate about 30–40% of the total energy when $V_{\mathrm{RBS},p}/V_p$ is in the following range:

$$0.70 \leqslant \frac{V_{\mathrm{RBS},p}}{V_p} \leqslant 0.90 \tag{9}$$

To calculate $V_{\mathrm{RBS},p}$ [Eq. (8)], it is suggested that the expected plastic moment at the RBS, $M_{\mathrm{RBS},p}$, be based on a cyclic strain hardening factor of 1.25 (Fig. 16). When a slab is present, this moment needs to be increased further by 10%.

Conclusions

A total of eight full-scale steel moment connection specimens that employed the RBS were tested. The test variables included the web connection type (bolted versus welded) and the panel zone strength. The following conclusions can be made based on the test results from this research and by others.

1. Both strong and medium panel zone specimens with a welded web connection exhibited satisfactory levels of connection ductility required of special moment-resisting frames. Specimens with a bolted web connection performed poorly due to premature brittle fracture of the beam flange at the weld access hole. The measured strain data appear to imply that the high incidence of base metal fracture in specimens with a bolted web connection is related to, at least in part, the increased demand in the beam flanges due to bolt slippage.
2. Welded-web specimens that were designed for a strong panel zone experienced more significant beam buckling and larger permanent distortions because inelastic action was concentrated in the RBS region. But using a very weak panel zone is also not favored due to concerns of potential weld fracture associated with the kinking of column flanges.
3. Test results from this study and by others showed that the panel zone could easily develop a plastic rotation of 0.01 rad without distressing the beam flange groove welds. Allowing the panel zone to deform inelastically at this level also reduces the magnitude of beam distortion (e.g., lateral torsional buckling) by about a half. A criterion for a balanced PZ strength [Eq. (9)] that improves the plastic rotation capacity while reduces the amount of beam distortion is presented.

Acknowledgment

Financial support to the first writer provided by the Research Institute of Industrial Science and Technology in Korea and the Korea Earthquake Engineering Research Center is gratefully acknowledged.

References

American Institute of Steel Construction (AISC). (1997 and 2002). *Seismic provisions for structural steel buildings*, American Institute of Steel Construction, Chicago.

Chen, S. J., Yeh, C. H., and Chu, J. M. (1996). “Ductile steel beam-to-column connections for seismic resistance.” *J. Struct. Eng.*, 122(11), 1292–1299.

Chi, B., and Uang, C.-M. (2002). “Cyclic response and design recommendations of reduced beam section moment connections with deep columns.” *J. Struct. Eng.*, 128(4), 464–473.

Choi, J. H., Stojadinovic, B., and Goel, S. C. (2000). “Development of free flange moment connection.” *Technical Rep. No. UMCEE 00-15*, Dept. of Civil and Environmental Engineering, Univ. of Michigan, Ann Arbor, Mich.

El-Tawil, S. (2000). “Panel zone yielding in steel moment connections.” *Eng. J.* 37(3), 120–131.

Engelhardt, M. D., Venti, M. J., Fry, G. T., Jones, S. L., and Holliday, S. D. (2000). “Behavior and design of radius cut reduced beam section connections.” *SAC/BD-00/17*, SAC Joint Venture, Sacramento, Calif.

Engelhardt, M. D., Winneberger, T., Zekany, A. J., and Potyraj, T. J. (1998). “Experimental investigations of dogbone moment connections.” *Eng. J.* 35(4), 128–139.

Iwankiw, N. (1997). “Ultimate strength consideration for seismic design of the reduced beam section (internal plastic hinge).” *Eng. J.* 34(1), 3–16.

Jones, S. L., Fry, G. T., and Engelhardt, M. D. (2002). “Experimental evaluation of cyclically loaded reduced beam section moment connections.” *J. Struct. Eng.*, 128(4), 441–451.

Kawano, A. (1984). “Inelastic behavior of low-rise frame based on a weak beam-to-column connection philosophy to earthquake motion.” *Proc., 8th World Conf. on Earthquake Engineering*, Vol. IV, San Francisco, 519–526.

Krawinkler, H. (1978). “Shear in beam-column joints in seismic design of steel frames.” *Eng. J.* 15(3), 82–91.

Krawinkler, H., Gupta, A., Medina, R., and Ruco, N. (2000). “Loading histories for seismic performance testing of SMRF components and assemblies.” *Rep. No. SAC/BD-00/10*, SAC Joint Venture, Sacramento, Calif.

Krawinkler, H., and Popov, E. P. (1982). “Seismic behavior of moment connections and joints.” *J. Struct. Div. ASCE*, 108(2), 373–391.

Plumier, A. (1997). “The dogbone: Back to the future.” *Eng. J.* 34(2), 61–67.

Ricles, J. M., Mao, C., Lu, L. W., and Fisher, J. W. (2002). “Inelastic cyclic testing of welded unreinforced moment connections.” *J. Struct. Eng.*, 128(4), 429–440.

Roeder, C. W. (2002). “General issues influencing connection performance.” *J. Struct. Eng.*, 128(4), 420–428.

SAC (2000). “Seismic design criteria for new moment-resisting steel frame construction.” *Rep. No. FEMA 350*, SAC Joint Venture, Sacramento, Calif.

Suita, K., Inoue, K., and Kanoh, N. (2002). “Strength and deformation of bolted beam-to-column connection accompanied by panel zone yield.” *Proc., 4th Taiwan–Japan–Korea Joint Seminar on Earthquake Engineering for Building Structures*, Seoul, Korea, 67–75.

Tsai, K. C., and Chen, W.-Z. (2000). “Seismic response of steel reduced

J. Struct. Eng., 2005, 131(12): 1854-1865

beam section to weak panel zone moment joints." *Proc., 3rd International Conf. STESSA 2000*, Montréal.
Tsai, K. C., and Popov, E. P. (1988). "Steel beam-column joints in seismic moment resisting frames." *EERC Rep. No. UCB/EERC-88/19*, Univ. of California, Berkeley, Calif.
Uang, C.-M. (1993). "An evaluation of two-level seismic design procedure." *Earthquake Spectra*, 9(1), 121–135.
Uang, C.-M., and Fan, C.-C. (2001). "Cyclic stability criteria for steel moment connections with reduced beam section." *J. Struct. Eng.*, 127(9), 1021–1027.
Yu, Q. S., Gilton, C., and Uang, C.-M. (2000). "Cyclic response of RBS moment connections: Loading sequence and lateral bracing effects." *SAC/BD-00/22*, SAC Joint Venture, Sacramento, Calif.
Zekioglu, A., Mozaffarian, H., Chang, K. L., and Uang, C.-M. (1997). "Designing after Northridge." *Modern Steel Constr.*, 37(3), 36–42.

J. Struct. Eng., 2005, 131(12): 1854-1865